Desalination and Water Treatment
www.deswater.com

doi: 10.1080/19443994.2016.1149740

57 (2016) 25242–25255
November

Taylor & Francis
Taylor & Francis Group

Diazo dye sorption by Ni-modified pumpkin husk

Abuzer Çelekli[a,*], Burcu Küçükgüner[a], Hüseyin Bozkurt[b]

[a]*Faculty of Art and Science, Department of Biology, University of Gaziantep, Gaziantep 27310, Turkey, Tel. +90 3423171925; emails: celekli.a@gmail.com (A. Çelekli), burcumsu_87@hotmail.com (B. Küçükgüner)*
[b]*Faculty of Engineering, Department of Food Engineering, University of Gaziantep, Gaziantep 27310, Turkey, email: hbozkurt@gantep.edu.tr*

Received 2 September 2015; Accepted 28 January 2016

ABSTRACT

The aim of this study was to investigate the potential of raw and modified pumpkin husk (*PH*) by loading of Ni^{2+} ions for removing Acid Black (AB 1). Surface structures of adsorbents were characterized by using Fourier Transform Infrared. Amine, amide, and carboxyl groups of *PH* played significant roles in the sorption process. Modification by Ni^{2+} ions led to increase in the sorption capacity of AB 1. AB 1 sorption on these adsorbents increased with decreasing particle size, adsorbent dose, solution pH, and temperature but increased with increasing contact time and initial dye concentration. Rapid sorption occurred in the first 5 min and equilibrium was reached within 50 min. Kinetic sorption data was well described by logistic model. Equilibrium data was best represented by Freundlich isotherm. Monolayer adsorption (maximum capacities of the *PH* as 227.62 mg g^{-1} and Ni-modified *PH* to adsorb AB 1 as 228.49 mg g^{-1}) was obtained when the experimental data were fitted to the Langmuir isotherm model. Activation energy and thermodynamic studies have shown that this process was physical, exothermic, and spontaneous. This study indicated that redundant *PH* had a great potential for the removal of AB 1 as an alternative eco-friendly process.

Keywords: Acid Black 1; Kinetic modeling; Modification; Pumpkin husk; Sorption

1. Introduction

Azo dyes are the largest and most versatile class of organic dyestuffs, approximately 60% of all dyestuffs, which is widely used in textile, leather, and paper industries [1]. Discharging of effluents from these industries into receiving water may cause adverse impacts on the ecosystems. The presence of dyes in water bodies reduces light penetration which can decrease photosynthetic activity and cause esthetic problems [1,2]. Also, many dyes or their metabolites in water bodies even at low concentration can cause variety of diseases and disorders in living organisms such as allergy, skin irritation, and cancer [3–6]. Complex aromatic structures of azo dyes make them more stable to the heat, oxidizing agents, photo-degradation, and biodegradation [7]. These dyes are classified as environmentally hazardous materials. Effluent contaminated by these dyes is sometimes used for irrigation of agricultural fields. By this way, recalcitrant compounds not only may affect growth of industrial plants, but also accumulated in them which can be transferred to organisms and humans [1,8]. Therefore,

*Corresponding author.

elimination of dyes from wastewater before discharging into water bodies is very important issue.

Several water treatment techniques such as ozonation, electro-coagulation/flocculation, chemical oxidation, ion-exchange, and photocatalytic degradation have been employed for the removal of dye. These processes usually involve some disadvantages, including complicated procedures, high energy demands, formation of by-products, and unsuitability of a wide range of dye-containing wastewaters. Therefore, there is an urgent need to develop an economic and effective method for removing dyes from aquatic systems in the world. Among treatment technologies, sorption process has received a lot of attention due to its simplicity, high efficiency, eco-friendly nature as well as the availability of a wide range of adsorbent with low cost [2,6,9,10]. So, studies for finding low-cost adsorbents with high adsorption capacities are still under improvement to decrease the adsorbent dosage and reduce the removal difficulties. In the recent years, many agricultural residues including coconut husk [11], maize cob [12], cashew nut shell [13], pistachio husk [14], Bengal gram seed husk [15], walnut husk [16], *Jatropha curcas* shells [17], and lentil straw [18] have been tested for removal of various dyes. Due to the huge annual production of agricultural wastes, it could therefore be used as a useful adsorbent. Effective disposal of agricultural wastes or by-products is an important work for environment protection and full utilization of resource.

Acid Black (AB 1) is a synthetic diazo dye containing –N=N– bonds and widely used in the textile and leather industries [6]. Another application of the AB 1 is as indicator to assist in the protein separation for chromatography and electrophoresis analyses [19]. AB 1 has the negative charge delocalized throughout the chromophoric system and has affinity toward the positively charged functional groups in materials.

A variety of chemical and physical methods are used for surface modification of adsorbents. The chemical methods involve metals or metal oxides impregnation, protonation, and grafting of amine groups. The physical method deals with thermal treatment of the adsorbent, thereby increasing its surface area and porosity. Impregnation of metals or metal oxides onto the adsorbent surface has a similar effect as surface protonation. The majority of metals can electrostatically bind to adsorbents by the attractive forces between the positively charged metal ions and negatively charged surface and/or by ligand exchange mechanism [20]. Thus, metal-loaded adsorbents get positively charged, which attract and adsorb anions such as anionic dye molecules. Adding metal can also increase the surface area and pore volume of adsorbents which in turn increase their sorption capacity of adsorbents [21].

Azo dyes are the most problematic dye, as they tend to pass through conventional treatment systems. Waste of pumpkin husk (*PH*) as an effective and low-cost adsorbent has not been previously used for removing of a diazo dye, AB 1. The use of waste for sorption purposes can play a significant role in helping solve disposal problem and protect environment. An attempt was made to enhance the adsorption capacity of *PH*, a waste, biomass by nickel ions pretreatment. Because of these reasons, redundant *PH* was chosen for this study. The aim of the present study was to investigate AB 1 sorption capacity of raw and modified *PH* by loading of Ni^{2+} ions as a function of particle size of the *PH* material, adsorbent dose, solution pH, contact time (kinetics at different temperatures were used to obtain the activation energy), and initial concentration of dye (isotherms at different temperatures were used to obtain the thermodynamic parameters). Furthermore, both the removal of Ni^{2+} ions and AB 1 by *PH* were included by taking same parameters. Enhanced sorption of AB 1 on modified *PH* with Ni^{2+} ions was explored under the aspects of sorption isotherms, sorption kinetics, and activation energy, isotherm, and thermodynamic studies.

2. Materials and methods

2.1. Materials

Pumpkin (*Cucurbita maxima*) husk (*PH*) was obtained from a field crop in the South East Anatolia. Dried *PH* (adsorbent) was ground in a mortar, sieved by use of different mesh sizes of sieves (63–125, 125–250, and 250–500 μm), and stored in air tight polyethylene bottle till use.

Dried *PH* was divided into two adsorbents; raw and pretreated. About 0.5 g L^{-1} of dried raw biomass *PH* was conducted to 200 mg L^{-1} Ni^{2+} solution for 60 min to obtain Ni-modified *PH* biomass. After then, pretreated *PH* biomass was separated via centrifugation at 5,000 rpm for 5 min, followed by successive washings with distilled water and re-centrifugation process. The dried Ni-modified adsorbent was stored in airtight polyethylene bottle for further studies. After the separation process, the residual Ni^{2+} concentration in solution was determined by using flame atomic adsorption spectrometer (Perkin Elmer AA 400, USA) at the wavelength of 232.0 nm. Raw and Ni-modified *PH* biomasses were used for the removal of AB 1 from aqueous solution.

2.2. Characterization

Zero point charge (pH_{zpc}) of *PH* was determined by use of powder addition method. A series of mixture solution (0.5 g adsorbent and 50 mL 0.1 M NaCl) in 100 mL conical flask was prepared at initial pH values ranging from 1 to 10, adjusted with 0.1 M HCl and/or 1.0 M NaOH solutions. Batches were agitated on orbital shaker at 150 rpm for 24 h and the final pH (pH_f) was measured at equilibrium. Value of pH_{zpc} was determined from the plot of pH_f against pH_i.

Infrared spectra of the raw and Ni-modified *PH* biomasses before and after the sorption process were taken using a Fourier transform infrared (FTIR) spectrometer equipped with an attenuated total reflection accessory (Perkin-Elmer Spectrum 100 FTIR-ATR Spectrometer).

The dye used in this study was C.I. AB 1 (CAS 1,064-48-8; $C_{22}H_{14}N_6Na_2O_9S_2$, MW = 616.49 g mol^{-1}; water solubility, 10 g L^{-1} (25°C); hazard codes, Xi, C, F) obtained from a local textile factory and used without further purification. The chemical structure and properties of this dye are given in Table 1. Stock dye solution (1 g L^{-1}) was prepared by dissolving accurately weighed quantity of AB 1 in distilled water. Dye solutions for the sorption process were prepared by the dilution of the stock dye solution with suitable volume of distilled water.

2.3. Sorption studies

The pH of solution was adjusted to desired value with 0.1 M HCl and/or 1.0 M NaOH solutions. Experiments were carried out in 250 mL conical flask containing 100 mL of the sorption solution (with desired dye concentration and pH) and desired amount of adsorbent. The flasks were agitated on an orbital shaker at 150 rpm.

AB 1 sorption of raw and Ni-modified *PH* as a function of particle size (63–125, 125–250, and 250–500 μm), adsorbent doses (0.5–4.0 g L^{-1}), solution pH (pH 1–9), contact time (0–50 min) were studied for kinetics at different temperatures (298, 308, and 318 K) to obtain the activation energy; and initial dye concentration (40–240 mg L^{-1}) were used for isotherms at different temperatures (298, 308, and 318 K) to obtain the thermodynamic parameters.

Sample solutions containing raw and Ni-modified *PH* biomass were prepared without dye (blank) at the same conditions and giving color of adsorbents into solution were determined by using spectrophotometer at 618 nm. It was found that they gave very little (negligible) color into solution.

During the sorption studies, withdrawn samples were centrifuged to precipitate suspended biomass at 6,000 rpm for 5 min. Residual AB 1 concentration in the supernatant was analyzed by the use of a spectrophotometer (Jenway 6305) at 618 nm. All of the

Table 1
General characteristics of AB 1

Name of dye	Acid black 1
Chemical formula	$C_{22}H_{14}N_6Na_2O_9S_2$
Molar mass	616.49 g mol^{-1}
Color index number	20,470
CAS number	1064-48-8
Hazard codes	Xi, C, F
Water solubility	10 g L^{-1} (25°C)
λ_{max}	618 nm
Chemical structure	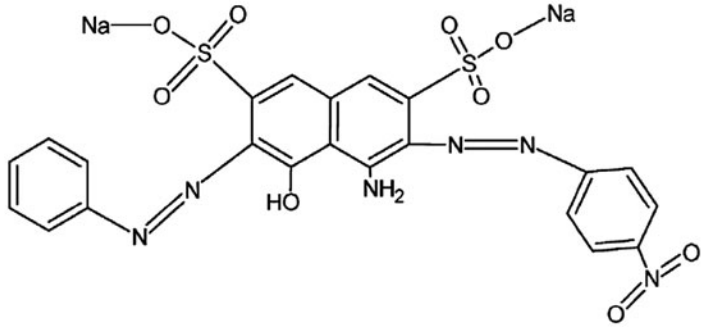

experiments were repeated two times and the mean values were used in data analyses.

In this study, q_t shows the amount of AB 1 adsorbed on *PH* at time t (mg g^{-1}) calculated by use of Eq. (1).

$$q_t = \frac{(C_o - C_t) \times V}{m} \quad (1)$$

where C_o and C_t represent the dye concentrations (mg L^{-1}) at initial and at t time, respectively. V is the volume of solution (L), and m is the mass of adsorbent (g L^{-1}).

Various theoretical equations (Table 2) were applied to experimental data in order to find a model which adequately predict kinetic or equilibrium data. The fitting procedure was performed by use of commercial computer software SigmaPlot version 11 (Systat Sofware, CA, USA) via the Marquardt–Levenberg algorithm. The applicability of models to describe the sorption process was validated by the coefficient of determination (R^2) and the sum of squares error (*SSE*) between experimental and predicted data from the models.

2.4. Desorption studies

PH was mixed with AB 1 solution and agitated at 150 rpm for 60 min. After the centrifugation process, absorbance of supernatant was measured for the determination of residual dye concentration in the solution. After then, obtained adsorbent was dried in the vacuum oven at 70°C for 24 h. The dye loaded *PH* was conducted with 50 mL of distilled water at alkaline pH values (pH 7, 8, 9, and 10) in 100 mL flaks, stirred on the orbital shaker at 150 rpm for 60 min. The amount of desorbed dye was determined from the released dye concentration in the solution. Four cycles of sorption–desorption were studied for the reuse of *PH*. Amount of desorbed dye was determined by using spectrophotometer at 618 nm. The percentage of desorbed dye from the adsorbent was calculated:

$$\text{Desorption}(\%) = \left(\frac{\text{mass of desorbed}}{\text{mass of adsorbed}}\right) \times 100 \quad (11)$$

3. Results and discussion

3.1. Characterization

The pH can control the sorption performance through different mechanisms including the magnitude of the electrostatic interactions to the changes of adsorbent surface properties and dye chemistry. Amphoteric adsorbent surfaces might be positively or negatively charged under different pH conditions. For that point, determination of pH_{zpc} of the adsorbent is important to assess the sorption mechanism. The pH_{zpc} of *PH* was found as 7.03 (Fig. 1), where electrostatic repulsion between *PH* and AB 1 molecules is minimum. Anion adsorption is more favorable when pH is lower than the value of pH_{zpc} due to the adsorbent surface getting positively charged.

Adsorption capacity depends on the chemical structure of the surface materials which consist of various functional groups such as amine, hydroxyl, carboxyl, carbonyl, sulfonate, and phosphate, which can bind with xenobiotic molecules.

FTIR–ATR analysis was conducted to obtain a better insight to the surface characteristics of the raw and Ni-modified *PH* before and after the sorption of *AB* 1. The spectra are given in Fig. 2(a)–(c). The dye-free raw *PH* had a broad and strong peak at 3,301 cm^{-1} (Fig. 2(a)), which is attributed to the NH_2 stretching vibrations in polysaccharides and proteins. This peak was shifted to 3,277 cm^{-1} (Fig. 2(b)) and 3,318 cm^{-1} (Fig. 2(c)) after the sorption of AB 1 and Ni^{2+} ions, respectively. This change could be due to the binding of the dye and/or metal with amino groups. There was no shift in the peaks at 2,917 cm^{-1} (–OH stretching), 2,850 cm^{-1} ($-CH_2$ symmetric stretching) in the spectra of the adsorbents, which did not participate in the sorption process. It is known that AB 1 has negative charge therefore it gives no interaction with negative ions. The spectrum of the raw *PH* had several strong peaks at 1,728 cm^{-1} (carbonyl (C=O) and carboxyl ($-COO^-$) groups), 1,645 cm^{-1} (−C=O amide, N–H bending, and –C-O stretching), 1,522 cm^{-1} (C–N stretching, N–H deformation), 1,370 cm^{-1} (C–H bending ($-CH_3$)), 1,233 cm^{-1} (–C–O stretching), and 1,027 cm^{-1} (groups of –C–O–C and –OH) [16,29–31]. These peaks were shifted to new values in the spectra (Fig. 2(a)–(c)), after the sorption process. These could be due to the formation of bonds between *PH* and AB 1 molecules and Ni^{2+} ions.

In order to find the effect of temperature on the sorption of AB 1 by Ni-modified *PH*, temperature values of 298, 308, and 318 K were performed and their FTIR spectra are given in Fig. 3(a)–(c), respectively. Results indicated that pretreated adsorbent with Ni^{2+} showed diverse broad peaks, after the sorption of AB 1. Peaks at 3,318, 1,634, and 1,228 cm^{-1} on Ni-modified *PH* under the 298 K (Fig. 3(a)) were shifted with increasing temperature of sorption solution (Fig. 3(b), (c)). Results indicated that sorption temperature affected amine, amide I, and –C–N stretching on *PH*

Table 2
Equations of models, error function, and activation energy

	Refs.	Equation
Kinetic models		
Pseudo second	[22]	$q_t = \frac{tq_e^2k}{tkq_e + 1}$ (2)
Logistic	[23]	$q_t = \frac{A}{\{1 + (\frac{x}{b})^c\}}$ (3)
Intra-particle diffusion	[24]	$q_t = k_i t^{0.5} + I$ (4)
Equilibrium models		
Langmuir	[25]	$\frac{C_e}{q_e} = \frac{1}{b_o q_L} + \frac{C_e}{q_L}$ (5)
Freundlich	[26]	$\log q_e = \log K_F + \frac{1}{n}\log C_e$ (6)
	[27]	$\ln q_e = \ln q_m - \beta\varepsilon^2$ (7)
D–R		$\varepsilon = RT\ln\left(1 + \frac{1}{C_e}\right)$ (8)
Error function		
Sums of squares error	[23]	$SSE = \sqrt{\frac{\sum(q_{exp} - q_{predict})^2}{N}}$ (9)
Activation energy		
Arrhenius	[28]	$\ln k = \ln A - \frac{E_a}{RT}$ (10)

could play a significant role on the formation of interactions between pretreated *PH* and AB 1 molecules. The overall spectral analysis strongly supported that the amino groups played a major role in the sorption of AB 1. Interaction between anionic dye molecules and adsorbent was also found for the sorption of Congo Red on cashew nut shell [13], AB 172 by *Pseudomonas* sp. strain DY1 [32], Lanaset Red G on *PH* [10], and AB 1 on *Nizamuddina zanardini* [33].

Adsorption of Ni^{2+} ions on *PH* was found as 54.12 mg g^{-1}, indicating that Ni-modified *PH* not only removed Ni^{2+} ions, but also had higher sorption capacity for AB 1.

3.2. Sorption

3.2.1. Effect of particle size

Three particle sizes of raw *PH* were conducted with 50 mg L^{-1} AB 1 solution and the plot is given on Fig. 4(a). The sorption capacity significantly decreased from 65.27 to 53.11 mg g^{-1} ($p < 0.01$), when particle size increased from 63–125 to 250–500 μm. The high sorption value was attributed to the fact that small particles had larger external surface area and better accessibility of dye molecules into pores than those of large particles. Increasing sorption capacity with decreasing particle size of various adsorbent was also observed [8,17,31,34]. Particle size of 63–125 μm had the highest sorption capacity, which was selected for further studies.

3.2.2. Effect of adsorbent dose

Fig. 4(b) shows the effect of adsorbent doses with 63–125 μm particle size on the sorption capacity of raw *PH*. It is apparent that sorption capacity significantly decreased with increasing the adsorbent dose ($p < 0.01$). This could be due to partial overlapping or aggregation of *PH* at higher biomass dose resulting in a decrease of total surface area and the availability of sorption site [5]. At 0.5 g L^{-1} of adsorbent dose, prevention of partial overlapping or aggregation of adsorbent cause to increase in the adsorbent surface areas and the number of available adsorption sites, which enhanced the sorption capacity of *PH*.

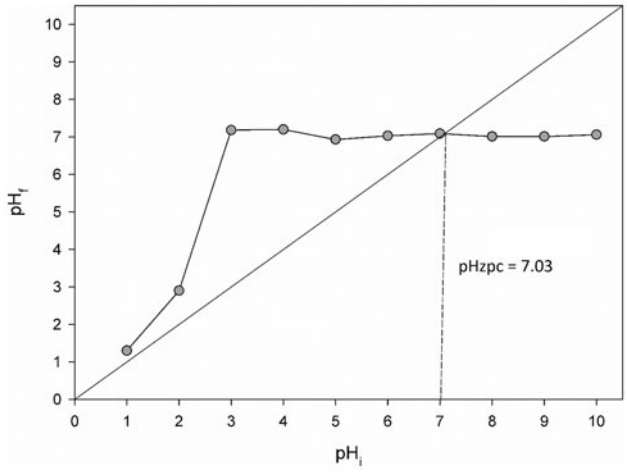

Fig. 1. Zero point of charge (pH_{zpc}) of pumpkin husk.

3.2.3. Effect of the solution pH

Effect of initial pH values from 1 to 9 on the sorption process is given on Fig. 4(c). As shown in Fig. 4(c), a tremendous reduction ($p < 0.01$) in the sorption value was observed, when the pH value of solution increases from 3 to 9. The surface of adsorbent is negatively charged, when solution pH is higher than pH_{zpc} causing to decrease sorption capacity, due to electrostatic repulsion. On the other hand, acidic condition (ranging in pH 1–3) supported the sorption capacity of *PH*. At $pH < pH_{zpc}$, the surface of adsorbent gets positively charged, absorbing more anionic dye (AB 1) molecules due to electrostatic force of attraction. The adsorption process of AB 1 strongly depended on the pH value of solution. In the present study, the highest sorption was found at pH 2. Sorption of AB1 by different macroalgae at acidic conditions were favored [33,35]. It could be very difficult to explain the sorption mechanism with respect to pH [36]. It could be due to a large number of variables involved in the sorption of dye such as the number and type of functional groups on the adsorbent surface, water chemistry etc. The pH 2 was selected for further studies.

Effects of particle size, adsorbent dose, and pH were also studied with Ni-modified *PH*. The similar results were also observed as they were obtained with raw *PH*.

3.2.4. Effect of contact time and temperature

Temperature is one of significant parameters governing the sorption process. The sorption capacity was found to increase with decrease in temperature for raw and Ni-modified *PH*, thereby indicating the process was exothermic in nature. This phenomenon can be a characteristic of a physical reaction between dye

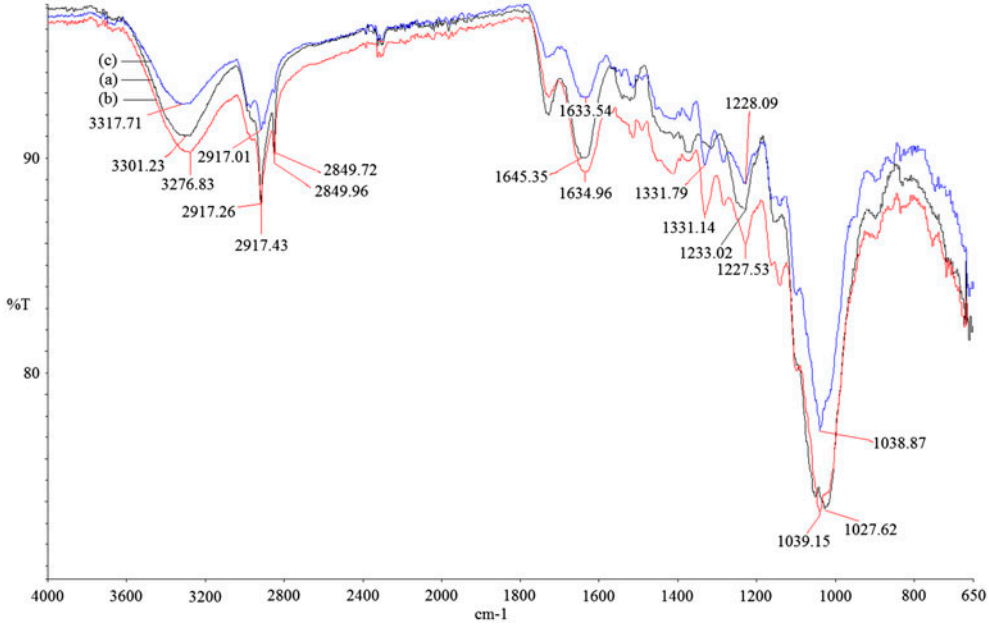

Fig. 2. FT-IR spectra of (a) the *PH*, (b) after the sorption of AB 1 on *PH*, (c) the Ni-modified *PH*, and (d) after the sorption of AB 1 on Ni-modified *PH*.

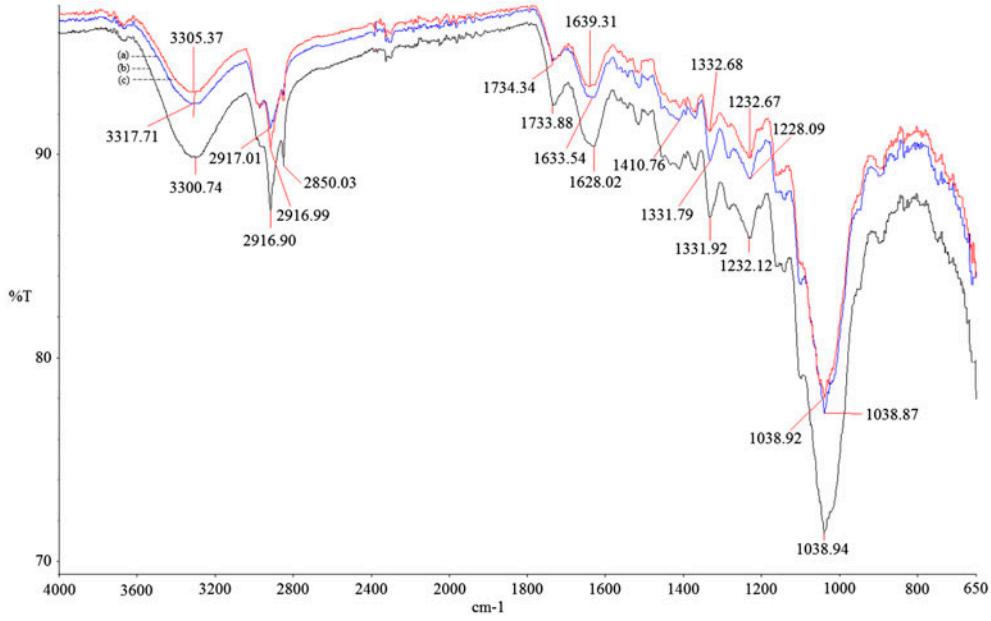

Fig. 3. After the sorption of AB 1 on Ni-modified *PH* at (a) 298, (b) 308, and (c) 318 K.

molecules and surface active groups of adsorbent being involved in the sorption process.

Contact time and initial dye concentrations played important role on the sorption process by raw and pretreated *PH*. Both *PH* biomasses showed similar patterns in the sorption curves and the sorption increased with increasing contact time ($p < 0.01$). The sorption process by Ni-modified *PH* (Fig. 5) was slightly faster than that of raw *PH*. It was clearly indicated that the sorption of AB 1 on both *PH* biomasses followed three-step processes, a rapid initial adsorption at the first 5 min followed by a period of slower uptake of AB 1 within 10–30 min and finally no significant uptake in 30–50 min. The first step could be attributed to the instantaneous utilization of the most readily available active sites on the *PH* surface as bulk diffusion. Second step, exhibiting additional sorption could be attributed to the diffusion of AB 1 from the surface film into the macro-pores of *PH* powders as pore diffusion or intra-particle diffusion. The last stage was an equilibrium stage, achieved within 30–50 min. This could be the consequence of saturation of functional groups of the exterior surface and entrance of dye molecules into the pores of the adsorbent. The rapid sorption has significant practical importance, as it facilitates smaller reactor volumes, ensuring high efficiency and economy. With regard to the sorption contact time, the present study indicated that both *PH* biomasses had great potential for the sorption of AB 1 compared to *Saccharomyces cerevisiae* [37], *Thelephora* sp. [38], *Cystoseira indica*, and *Gracilaria persica* [35], and *N. zanardinii* [33].

3.2.4.1. Kinetic (mathematical models). Pseudo-second-order kinetic, Logistic, Avrami, Elovich, and intra-particle diffusion models (Table 2) were used to investigate sorption behavior of AB 1 by raw and Ni-modified *PH*.

Predictive modeling of sorption kinetics of AB 1 by both adsorbents at 298 K is summarized in Table 3. Predicted parameters from the kinetic models at 308 and 318 K were also calculated but are not presented here. All studied kinetic models were well fitted to the experimental data. However, values of R^2 (≥ 0.999) and *SSE* (0.091–1.767) suggest that the logistic and Avrami models represent better (Table 3). Besides, it was clearly indicated that outputs (q_{pred}) of Logistic (Fig. 5) and Avrami (not shown) models agreed well with the corresponding targets (q_{exp}) within experimental ranges. Well-fitting results were also found in previous studies for Logistic model, in which for removing of Lanaset Red G on *Chara contraria* [39] and on walnut husk [16] and for Avrami model, in which for the sorption of Reactive Red M-2BE by active carbon [40].

Maximum sorption of AB 1 obtained from Logistic model was 196.54 and 225.84 mg g^{-1} for raw and Ni-modified *PH*, respectively (Table 3). Ni^{2+}-loading increased the sorption capacity of *PH* about 15 % comparing to raw form. There was not only sorption of

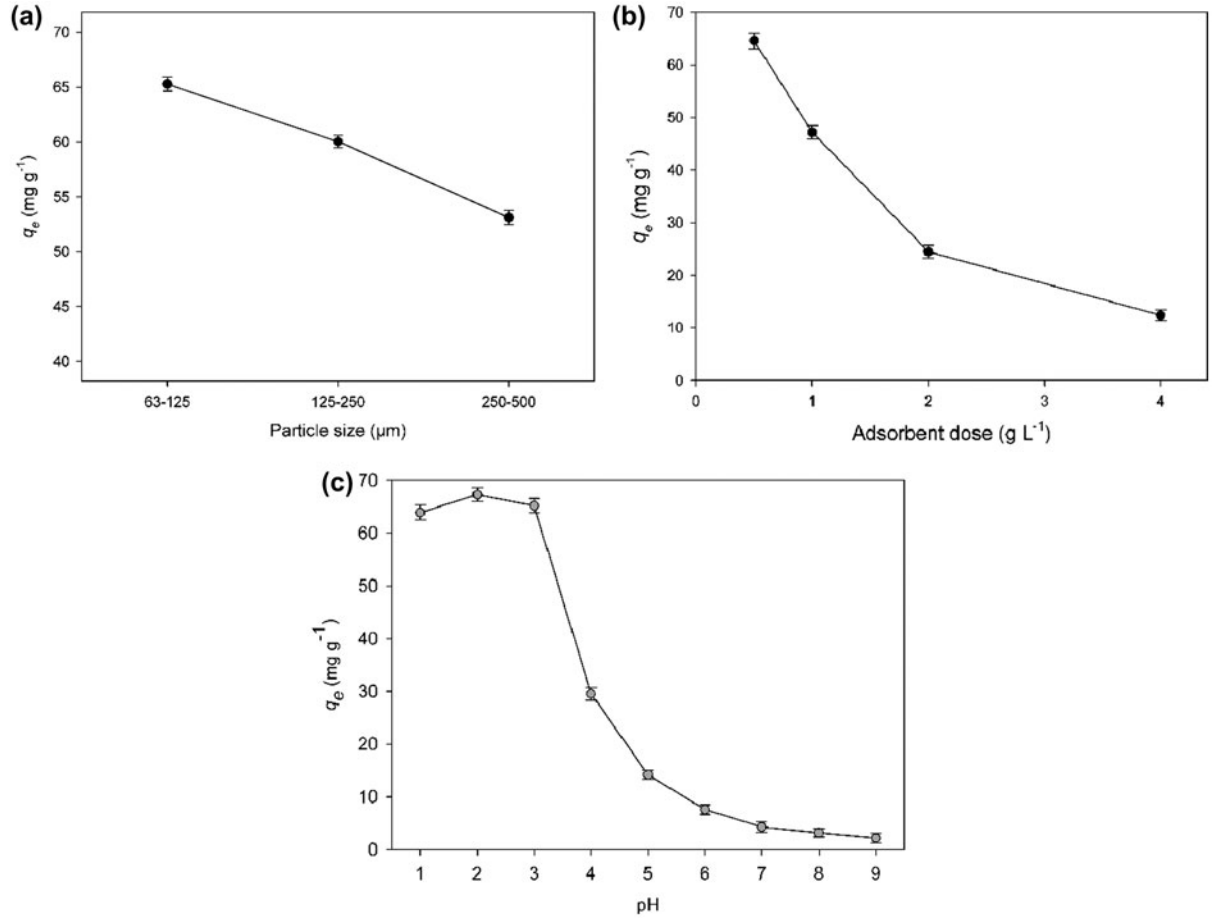

Fig. 4. Effects of (a) particle size, (b) adsorbent dose, (c) initial pH on the sorption of AB 1 on *PH* at 50 mg L^{-1}.

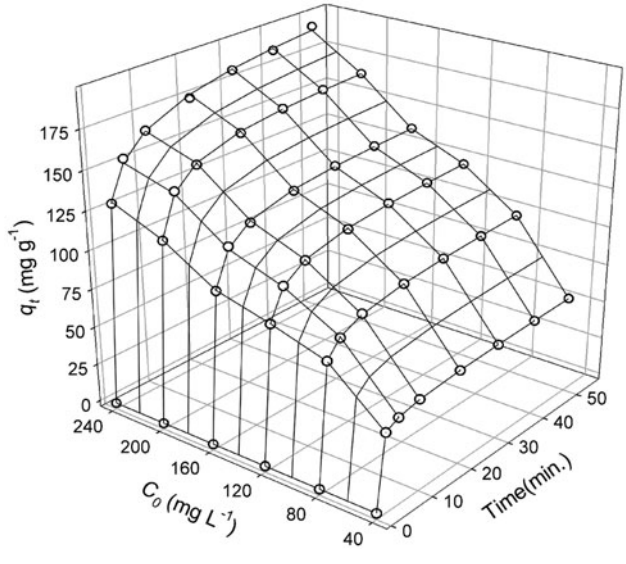

Fig. 5. Effect of contact time and initial azo dye concentration on the sorption by Ni-modified *PH* at pH 2. Comparison between experimental points (circle) and fitted curves by Logistic model with mesh lines.

Ni^{2+} ions, but also higher sorption of AB 1 by pretreated *PH* with Ni^{2+} was obtained than those of raw *PH*. The sorption rate (μ, mg g^{-1} min^{-1}) of logistic model increased with decreasing temperature, indicating that the sorption kinetic of AB 1 by *PH* was exothermic in nature.

Intra-particle diffusion model [24] was fitted to experimental data to evaluate the sorption mechanisms. Intra-particle diffusion is the rate-controlling mechanism by use of a plot of q_t and $t^{0.5}$. The q_t vs. $t^{0.5}$ graphs (not shown) of both raw and Ni-modified *PH* indicated that two intercepting lines could involve in sorption process of *AB* 1 on both raw and Ni-modified *PH*. Predominant first step could be attributed to rapid diffusion of *AB* 1 molecules through solution to the external surface of *PH* powders and diffusion of dye molecules through boundary layer to the surface of adsorbent. The last step could be attributed to the equilibrium period, which intra-particle diffusion started to slow down due to extremely low residual dye concentration in solution. In

the present study, the plots did not pass through the origin as a straight line, indicating that the intra-particle diffusion is involved in the sorption process, but is not the only rate controlling step.

3.2.4.2. Activation energy. Arrhenius equation (Table 2) was used to determine activation energy (E_a) for the sorption of AB 1 by raw and Ni-modified *PH*. From that point, pseudo second rate constant (k) and logistic sorption rate constant (μ) were applied to Arrhenius equation.

Magnitude of E_a gives information about sorption type either physical or chemical. Physical sorption process is reversible, requires low energy in ranging from 5 to 40 kJ mol^{-1}. Conversely, strong forces and high activation energy is required (between 40 and 800 kJ mol^{-1}) for chemical sorption. Activation energy for the sorption of AB 1 by raw *PH* was found as

Table 3
Kinetic parameters for the sorption of AB 1 on raw and Ni-modified *PH* (pH 2; particle size, 63–125 μm; m = 0.5 g L^{-1}, 298 K, and t = 50 min)

		Unit	Raw *PH*					
	C_0	(mg L^{-1})	40	80	120	160	200	240
Pseudo-second	q_{exp}	(mg g^{-1})	57.3	100.55	124.97	139	166.58	189.7
	k	(g mg^{-1} min^{-1})	0.0278	0.013	0.008	0.007	0.006	0.005
	q_{pred}	(mg g^{-1})	56.71	100.37	126.39	140.65	168.48	192.08
	R^2		0.996	0.9975	0.9992	0.9993	0.9993	0.9993
	SSE		1.137	1.576	1.093	1.192	1.430	1.567
	μ	(mg g^{-1} min^{-1})	22.168	37.218	42.675	46.824	56.810	63.369
	A	(mg g^{-1})	68.69	109.34	130.38	143.9	173.07	196.54
	R^2		0.9999	0.9999	0.9999	0.9997	0.9998	0.9997
	SSE		0.103	0.297	0.390	0.812	0.780	1.013
Elovich	$\alpha \times 10^{10}$	(mg g^{-1} min^{-1})	0.8	0.8	0.8	0.8	0.8	0.8
	β	(g mg^{-1})	0.558	0.313	0.252	0.227	0.187	0.164
	R^2		0.9832	0.974	0.9522	0.9487	0.9524	0.9466
	SSE		2.327	5.091	8.645	9.966	11.496	13.881
Avrami	q_{av}	(mg g^{-1})	62.69	103.57	125.82	139.4	167.44	190.23
	k_{av}	(min^{-1})	1.293	1.067	0.679	0.649	0.679	0.626
	n_{av}	(mg g^{-1} min^{-1})	0.217	0.316	0.437	0.456	0.443	0.461
	R^2		0.9999	0.9999	0.9997	0.9993	0.9995	0.9994
	SSE		0.091	0.253	0.644	1.160	1.169	1.520
			Ni-modified *PH*					
Pseudo-second	q_{exp}	(mg g^{-1})	59.2	103.42	127.39	141.83	169.45	192.9
	k	(g mg^{-1} min^{-1})	0.0322	0.0132	0.0079	0.0069	0.0059	0.0051
	q_{pred}	(mg g^{-1})	58.65	103.19	128.75	143.41	171.29	188.84
	R^2		0.9977	0.9976	0.9992	0.9993	0.9993	0.9944
	SSE		0.899	1.598	1.118	1.213	1.455	4.426
Logistic	μ	(mg g^{-1} min^{-1})	23.67	38.65	43.88	48.24	58.24	64.93
	A	(mg g^{-1})	65.61	112.34	132.87	146.81	176.02	225.84
	R^2		1.0000	0.9999	0.9999	1.0000	1.0000	0.9993
	SSE		0.092	0.299	0.387	0.807	0.775	1.618
Elovich	$\alpha \times 10^{10}$	(mg g^{-1} min^{-1})	0.8	0.8	0.8	0.8	0.8	0.8
	β	(g mg^{-1})	0.533	0.303	0.247	0.221	0.184	0.167
	R^2		0.9902	0.9764	0.9549	0.9517	0.9548	0.9501
	SSE		1.838	4.989	8.560	9.868	11.395	13.214
Avrami	q_{av}	(mg g^{-1})	62.01	106.53	128.28	142.27	170.36	207.28
	k_{av}	(min^{-1})	2.411	1.152	0.707	0.676	0.704	0.484
	n_{av}	(mg g^{-1} min^{-1})	0.233	0.310	0.432	0.450	0.438	0.288
	R^2		1.0000	0.9999	0.9998	0.9993	0.9995	0.9991
	SSE		0.096	0.259	0.635	1.150	1.159	1.767

−8.431 to −16.859 kJ mol^{-1} by use of k and μ, respectively. For Ni-modified *PH*, −9.518 to −17.079 kJ mol^{-1} were found by use of k and μ, respectively. Magnitude of E_a indicated that the sorption of AB 1 on both raw and Ni-modified *PH* was physical character and exothermic.

3.2.5. Effect of initial dye concentration and temperature

Fig. 5 showed that increasing initial dye concentration significantly increased ($p < 0.01$) the uptake of AB 1 by Ni-modified *PH*. This could be consequence of increase in the driving force for mass transfer, in agreement with results of previous studies [8,10]. Additionally, the increase in initial dye concentration enhanced probability of interaction between dye molecules and adsorbent. The sorption capacity was found to increase with decrease in temperature for raw and Ni-modified *PH* for each AB 1 concentrations.

3.2.5.1. Isotherms (mathematical models). Langmuir, Freundlich, and Dubinin–Radushkevish (D–R) isotherms (Table 2) were used to describe the equilibrium data of sorption between adsorbed AB1 on the *PH* (q_{eq}) and unabsorbed AB 1 in solution (C_{eq}).

Fitting results of equilibrium models are given in Table 4. Monolayer sorption capacities of raw and Ni-modified *PH* increased, when temperature was decreased from 318 to 298 K. This indicated that the sorption process is an exothermic. Langmuir and Freundlich isotherms had high correlation coefficient for describing the sorption of AB 1 by both *PH* biomasses (Table 4). However, Freundlich model had lower error values as *SSE* = 0.0139–0.0233 and 0.0143–0.0223 than those of mentioned isotherms for both raw and Ni-modified *PH*, respectively. Besides, the plots of log q_e vs. log C_e (Fig. 6) indicated applicability of Freundlich model, showed well agreement with the q_{exp} values for Ni-modified *PH*, respectively. Thus, it could be concluded that the sorption process could occur as a heterogeneous phenomenon for both *PH* biomasses.

Freundlich isotherm model [26] is valid for multilayer adsorption and is derived by assuming a heterogeneous surface with interaction between adsorbed molecules with a non-uniform distribution of sorption heat over the surface. Freundlich constant value ($n > 2$) also indicated favorable the sorption process. Ni-modified *PH* had greater adsorption capacity (K_F) values (15.884–23.065) than those of raw *PH* (14.665–20.571). From that point, both PH powders had the greater adsorption capacity for AB 1 than those of previous studies [33,35].

Adsorption capacities of azo dyes on various adsorbents were compared and results are given in Table 5. In this study, monolayer sorption capacities of raw and Ni-modified *PH* obtained from Langmuir model were found to be 227.62 and 228.49 mg g^{-1}, respectively (Table 4). Both adsorbents of *PH* had a great potential for the sorption of AB 1 comparing to the sorption of the same dye on *Saccharomyces cerevisiae* [37], *Thelephora* sp. [38], *C. indica* and *G. persica* [35], and *N. zanardinii* [33]. This satisfactory sorption capacity of *PH* might be due to difference in type and amount of functional groups on their structures and sorption mechanisms of various adsorbents and

Table 4
Values of isotherm parameters for the sorption of AB 1 on raw and Ni-modified *PH*. (pH 2; particle size, 63–125 μm; m = 0.5 g L^{-1}, C_0 = 40–240 mg L^{-1}, 298 K, and t = 50 min)

		Raw *PH*			Ni-modified *PH*		
	Temp. (K)	298	308	318	298	308	318
Langmuir	q_L	227,62	193,68	171,84	228,49	193,98	176,58
	b_o	0.0242	0.0195	0.0192	0.0268	0.0213	0.0199
	R_L	0.2530	0.2959	0.2992	0.2342	0.2779	0.2917
	R^2	0.9618	0.9653	0.9673	0.9619	0.9642	0.9642
	SSE	0.0412	0.0501	0.0572	0.0413	0.0514	0.0623
Freundlich	K_F	20.571	15.779	14.665	23.065	17.495	15.884
	n	2.267	2.225	2.306	2.371	2.327	2.377
	R^2	0.9811	0.9889	0.9917	0.9816	0.9903	0.9912
	SSE	0.0233	0.0169	0.0139	0.0223	0.0170	0.0143
D–R	q_m	148.44	122.97	111.03	150.68	125.08	112.06
	β	22.66	30.99	32.96	18.77	25.84	28.56
	R^2	0.8295	0.7861	0.7863	0.8239	0.7716	0.7589
	SSE	0.1615	0.1706	0.1614	0.1610	0.1734	0.1696

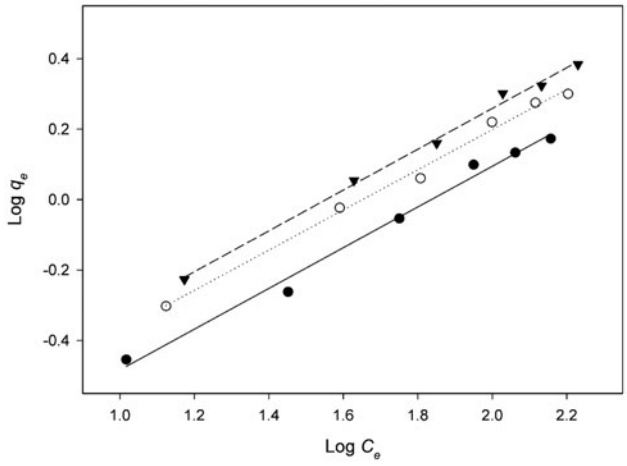

Fig. 6. Freundlich isotherm for sorption of AB 1 on Ni-modified *PH* at different temperatures (pH 2; particle size, 63–125 μm; m = 0.5 g L^{-1}, C_0 = 40–240 mg L^{-1}, and t = 50 min).

experimental conditions. Moreover, Ni-modified *PH* not only removed Ni^{2+} ions (54.12 mg g^{-1}), but also had higher sorption capacity for AB 1 (228.49 mg g^{-1}) than those of raw *PH*.

In order to find sorption type either physical or chemical, mean free energy (E (kJ mol^{-1})) could be used and estimated from D–R model, using following relationship ($E = 1/\sqrt{2\beta}$), where β is a constant related to sorption energy. When E is lower than 8 kJ mol^{-1}, it depicts physical sorption, while E is between 8 and 16 kJ mol^{-1}, it indicates chemical sorption [42]. In the present study, values of E for raw and Ni-modified *PH* were found to be 0.13 and 0.14 kJ mol^{-1}, respectively. Both mean free energy values were lower than 8 kJ mol^{-1}, which indicated the sorption process was physical.

3.2.5.2. Thermodynamics. In order to evaluate the sorption process whether it is spontaneous or not and exothermic or endothermic, thermodynamic parameters [standard free energy changes (ΔG°, kJ mol^{-1}), enthalpy changes (ΔH°, kJ mol^{-1}), and entropy changes (ΔS°, J mol^{-1} K^{-1})] were determined by following equations:

$$\Delta G^\circ = -RT\ln(K_L) \quad (12)$$

$$\Delta G^\circ = \Delta H^\circ - T\Delta S^\circ \quad (13)$$

where R is the universal gas constant (8.314 J mol^{-1} K), T is temperature (K), and K_L is Langmuir constant (L mol^{-1}). Values of ΔH° and ΔS° can be determined from the slope and intercept of a plot of $ln\ K_L$ versus $1/T$ (not shown). Results are given in Table 6. Negative value of ΔH° indicated that the sorption process was exothermic. Variation in free energy between −20 and 0 kJ mol^{-1} indicated physical sorption, whereas the energy ranging from −80 to −400 kJ mol^{-1} shows chemical sorption. Values of ΔG° varied from −23.057 to −24.891 kJ mol^{-1}, indicated that the sorption process for both adsorbents was mainly physical. Besides, negative value of ΔG° indicated this process is being feasible and spontaneous nature of sorption.

3.3. Desorption

Desorption studies were required to recover adsorbent for the reuse and evaluate the mechanism of the

Table 5
The natural forms of agricultural waste and its dye adsorption capacities

Adsorbent	Adsorbate	q_{max}	Refs.
Cashew nut shell	Congo red	5.18	[13]
Jujuba seed	Congo red	55.56	[15]
Bengal gram seed husk	Congo red	41.66	[15]
Pistachio husk	Reactive red 120	324.88	[14]
Jatropha curcas shells	Reactive red 120	65.63	[17]
Pumpkin husk *C. moschata*	Reactive red 120	98.61	[41]
Pumpkin husk *C. moschata*	Lanaset red G	436.28	[10]
Saccharomyces cerevisiae	Acid black 1	11.60	[37]
Thelephora sp.	Acid black 1	11.00	[38]
Cystoseira indica	Acid black 1	8.34	[35]
Gracilaria persica	Acid black 1	9.18	[35]
Nizamuddina zanardinii	Acid black 1	29.79	[33]
raw *PH Cucirbita maxima*	Acid black 1	227.50	The present study
Ni-modified *PH C. maxima*	Acid black 1	228.49	The present study

Table 6
Thermodynamic parameters for sorption process of dye on adsorbent at different temperatures (C_0 = 30–180 mg L^{-1}, particle size = 45–63 μm, pH 2, m = 0.5 g L^{-1}, and t = 90 min)

	T (K)	ΔG° (kJ mol^{-1})	ΔH° (kJ mol^{-1})	ΔS° (kJ mol^{-1} K^{-1})
Raw *PH*	298	−23.810	−9.035	0.049
	308	−23.057		
	318	−23.797		
Ni-modified *PH*	298	−24.063	−11.662	0.041
	308	−24.283		
	318	−24.891		

sorption process. Strong binding (e.g. covalent and ionic bindings) and weak binding (e.g. Van der Waals' forces and a dipole–dipole interaction) can be formed between the adsorbent surface and dye molecules which directly affect reversibility of sorption process.

Alkaline solutions (pH 7, 8, 9, and 10) as desorption agents were used to desorb dye from AB 1-loaded *PH*. The highest desorption (83%) was found at pH 10 and this rate decreased with decreasing pH value. This might be due to enhancement of negatively charged sites at high pH value which increased electrostatic repulsion, supported desorption of anionic dye molecules. AB 1-loaded *PH* had remarkable desorption ability, which was higher than that of pine cone [43], and lentil straw [18] for anionic dyes. Four cycles of sorption–desorption were studied for the reuse of *PH*. Desorption efficiency of *PH* was found as 76.2% after the fourth cycles. Interactions between AB 1 molecules and *PH* surface were mainly weak binding forces, which could facilitate high desorption efficiency and generated adsorbent. Besides, results of activation energy and thermodynamic parameters supported desorption studies. The regenerated adsorbent indicated satisfying sorption capability toward AB 1, which could be used as a potential adsorbent for treatment systems.

4. Conclusions

The potential of raw and modified *PH* by loading of Ni^{2+} ions for removing AB 1 were investigated as a function of particle size, adsorbent dose, solution pH, contact time, initial dye concentration, and temperature. FTIR indicated that amine, amide, and carboxyl groups of *PH* played significant roles in the sorption process. Modification by Ni^{2+} ions led to increase in the sorption capacity of AB 1. AB 1 sorption on these adsorbents increased with decreasing particle size, adsorbent dose, solution pH, and temperature but increased with increasing contact time, and initial dye concentration. Rapid sorption occurred during the first 5 min and equilibrium was reached within 50 min. Kinetic sorption data was well described by logistic model, whereas equilibrium data was best represented by Freundlich isotherm. Maximum adsorption capacities of AB 1 were found as 227.62 mg g^{-1} on the *PH* and as 228.49 mg g^{-1} on Ni-modified *PH*, derived from the Langmuir isotherm. The process was physical, exothermic, and spontaneous. The present study revealed that especially Ni-modified *PH* had a great potential for the removal of AB 1 as an alternative eco-friendly process.

Acknowledgments

Authors thank to Scientific Research Projects Executive Council of University of Gaziantep and DPT (T.R. Prime Ministry State Planning Organization).

Nomenclature

A — asymptote value from Logistic model
b_o — Langmuir constant (L mg)
β — constant related to sorption energy of D–R model (mol^2 kJ^{-2})
C_e — equilibrium dye concentration (mg L^{-1})
C_o — initial dye concentration (mg L^{-1})
k — pseudo-second-order rate constant (g mg min^{-1}))
K_F — Freundlich adsorption capacity [(mg g^{-1}) (mg $L^{-1})^{-\frac{1}{n}}$]
n — Freundlich adsorption intensity
PH — Pumpkin husk
q_e — amount of adsorbed dye at equilibrium (mg g^{-1})
q_{exp} — experimental amount of adsorbed dye at equilibrium (mg g^{-1})
q_{pred} — predicted amount of adsorbed at equilibrium (mg g^{-1})
q_m — the monolayer adsorption capacity of Langmuir model (mg g^{-1})

q_t — amount of adsorbed dye per unit of biomass at time t (mg g^{-1})
R^2 — determination coefficient
t — time (min)
SSE — The sum of square error
N — number of data point

References

[1] R.G. Saratalea, G.D. Sarataleb, J.S. Chang, S.P. Govindwar, Bacterial decolorization and degradation of azo dyes: A review, J. Taiwan Inst. Chem. Eng. 42 (2011) 138–157.
[2] V.K. Gupta, R. Kumar, A. Nayak, T.A. Saleh, M. Barakat, Adsorptive removal of dyes from aqueous solution onto carbon nanotubes: A review, Adv. Colloid Interface Sci. 193-194 (2013) 24–34.
[3] A. Çelekli, M. Yavuzatmaca, H. Bozkurt, Kinetic and equilibrium studies on the adsorption of reactive red 120 from aqueous solution on *Spirogyra majuscula*, Chem. Eng. J. 152 (2009) 139–145.
[4] V. Gupta, Application of low-cost adsorbents for dye removal—A review, J. Environ. Manage. 90 (2009) 2313–2342.
[5] S. Dawood, T.K. Sen, Removal of anionic dye Congo red from aqueous solution by raw pine and acid-treated pine cone powder as adsorbent: Equilibrium, thermodynamic, kinetics, mechanism and process design, Water Res. 46 (2012) 1933–1946.
[6] M.A.M. Salleh, D.K. Mahmoud, W.A.W.A. Karim, A. Idris, Cationic and anionic dye adsorption by agricultural solid wastes: A comprehensive review, Desalination 280 (2011) 1–13.
[7] M. Solís, A. Solís, H.I. Pérez, N. Manjarrez, M. Flores, Microbial decolouration of azo dyes: A review, Process Biochem. 47 (2012) 1723–1748.
[8] J. Paul, A.A. Kadam, S.P. Govindwar, P. Kumar, L. Varshney, An insight into the influence of low dose irradiation pretreatment on the microbial decolouration and degradation of Reactive Red-120 dye, Chemosphere 90 (2013) 1348–1358.
[9] A. Bhatnagar, M. Sillanpää, A review of emerging adsorbents for nitrate removal from water, Chem. Eng. J. 168 (2011) 493–504.
[10] A. Çelekli, H. Bozkurt, Predictive modeling of an azo metal complex dye sorption by pumpkin husk, Environ. Sci. Pollut. Res. 20 (2013) 7355–7366.
[11] V.K. Gupta, R. Jain, M. Shrivastava, Adsorptive removal of Cyanosine from wastewater using coconut husks, J. Colloid Interface Sci. 347 (2010) 309–314.
[12] G. Sonawane, V. Shrivastava, Kinetics of decolourization of malachite green from aqueous medium by maize cob (*Zea maize*): An agricultural solid waste, Desalination 247 (2009) 430–441.
[13] P. Senthil Kumar, S. Ramalingam, C. Senthamarai, M. Niranjanaa, P. Vijayalakshmi, S. Sivanesan, Adsorption of dye from aqueous solution by cashew nut shell: Studies on equilibrium isotherm, kinetics and thermodynamics of interactions, Desalination 261 (2010) 52–60.
[14] A. Çelekli, M. Yavuzatmaca, H. Bozkurt, Modeling the removal of reactive red 120 on pistachio husk, Clean 38 (2010) 173–180.
[15] S. Reddy, L. Sivaramakrishna, A. Varada, The use of an agricultural waste material, Jujuba seeds for the removal of anionic dye (Congo red) from aqueous medium, J. Hazard. Mater. 203-204 (2012) 118–127.
[16] A. Çelekli, S.S. Birecikligil, F. Geyik, H. Bozkurt, Prediction of removal efficiency of Lanaset Red G on walnut husk using artificial neural network model, Bioresour. Technol. 103 (2012) 64–70.
[17] L.D.T. Prola, E. Acayanka, E.C. Lima, C.S. Umpierres, J.C.P. Vaghetti, W.O. Santos, S. Laminsi, P.T. Djifon, Comparison of Jatropha curcas shells in natural form and treated by non-thermal plasma as biosorbents for removal of reactive red 120 textile dye from aqueous solution, Ind. Crop Prod. 46 (2013) 328–340.
[18] A. Çelekli, B. Tanrıverdi, H. Bozkurt, Lentil Straw: A novel adsorbent for removing of hazardous dye-sorption behavior studies, Clean 40 (2012) 515–522.
[19] F.J. Green, The Sigma-Aldrich handbook of stains, dyes and indicators, Aldrich Chemical Co., Milwaukee, WI, 1990.
[20] P. Loganathan, S. Vigneswaran, J. Kandasamy, R. Naidu, Cadmium sorption and desorption in soils: A review, Crit. Rev. Environ. Sci. Technol. 42 (2012) 489–533.
[21] H. Demiral, G. Gündüzoğlu, Removal of nitrate from aqueous solutions by activated carbon prepared from sugar beet bagasse, Bioresour. Technol. 101 (2010) 1675–1680.
[22] Y.-S. Ho, G. McKay, Pseudo-second order model for sorption processes, Process Biochem. 34 (1999) 451–465.
[23] A. Çelekli, M. Yavuzatmaca, H. Bozkurt, An eco-friendly process: Predictive modelling of copper adsorption from aqueous solution on *Spirulina platensis*, J. Hazard. Mater. 173 (2010) 123–129.
[24] W. Weber, J. Morris, Kinetics of adsorption on carbon from solution, J. Sanit. Eng. Div. Am. Soc. Civ. Eng. 89 (1963) 31–60.
[25] I. Langmuir, The adsorption of gases on plane surfaces of glass, mica and platinum, J. Am. Chem. Soc. 40 (1918) 1361–1403.
[26] H. Freundlich, Over the adsorption in solution, J. Phys. Chem. 57 (1906) 1100–1107.
[27] M. Dubinin, L. Radushkevich, Equation of the characteristic curve of activated charcoal, USSR Phys. Chem. Sect. 55 (1947) 331–337.
[28] T. Anirudhan, P. Radhakrishnan, Thermodynamics and kinetics of adsorption of Cu(II) from aqueous solutions onto a new cation exchanger derived from tamarind fruit shell, J. Chem. Thermodyn. 40 (2008) 702–709.
[29] A. Çelekli, G. İlgün, H. Bozkurt, Sorption equilibrium, kinetic, thermodynamic, and desorption studies of Reactive Red 120 on *Chara contraria*, Chem. Eng. J. 191 (2012) 228–235.
[30] J. Yang, K. Qiu, Preparation of activated carbons from walnut shells via vacuum chemical activation and their application for methylene blue removal, Chem. Eng. J. 165 (2010) 209–217.
[31] F. Kaouah, S. Boumaza, T. Berrama, M. Trari, Z. Bendjama, Preparation and characterization of activated carbon from wild olive cores (oleaster) by

H_3PO_4 for the removal of Basic Red 46, J. Cleaner Prod. 54 (2013) 296–306.
[32] L.-N. Du, B. Wang, G. Li, S. Wang, D.E. Crowley, Y.-H. Zhao, Biosorption of the metal-complex dye Acid Black 172 by live and heat-treated biomass of *Pseudomonas* sp. strain DY1: Kinetics and sorption mechanisms, J. Hazard. Mater. 205–206 (2012) 47–54.
[33] A. Esmaeli, M. Jokar, M. Kousha, E. Daneshvar, H. Zilouei, K. Karimi, Acidic dye wastewater treatment onto a marine macroalga, *Nizamuddina zanardini* (Phylum: Ochrophyta), Chem. Eng. J. 217 (2013) 329–336.
[34] E. Daneshvar, M. Kousha, M. Jokar, N. Koutahzadeh, E. Guibal, Acidic dye biosorption onto marine brown macroalgae: Isotherms, kinetic and thermodynamic studies, Chem. Eng. J. 204–206 (2012) 225–234.
[35] M. Kousha, E. Daneshvar, H. Dopeikar, D. Taghavi, A. Bhatnagar, Box-Behnken design optimization of Acid Black 1 dye biosorption by different brown macroalgae, Chem. Eng. J. 179 (2012) 158–168.
[36] Z. Aksu, S. Tezer, Biosorption of reactive dyes on the green alga *Chlorella vulgaris*, Process Biochem. 40 (2005) 1347–1361.
[37] M. Šafaříková, L. Ptáčková, I. Kibrikova, I. Šafařík, Biosorption of water-soluble dyes on magnetically modified *Saccharomyces cerevisiae* subsp. *uvarum* cells, Chemosphere 59 (2005) 831–835.
[38] K. Selvam, K. Swaminathan, K.-S. Chae, Decolourization of azo dyes and a dye industry effluent by a white rot fungus *Thelephora* sp., Bioresour. Technol. 88 (2003) 115–119.
[39] A. Çelekli, B. Tanrıverdi, H. Bozkurt, Predictive modeling of removal of Lanaset Red G on *Chara contraria*; kinetic, equilibrium, and thermodynamic studies, Chem. Eng. J. 169 (2011) 166–172.
[40] F.M. Machado, C.P. Bergmann, T.H. Fernandes, E.C. Lima, B. Royer, T. Calvete, S.B. Fagan, Adsorption of reactive red M-2BE dye from water solutions by multi-walled carbon nanotubes and activated carbon, J. Hazard. Mater. 192 (2011) 1122–1131.
[41] A. Çelekli, F. Çelekli, E. Çiçek, H. Bozkurt, Predictive modeling of sorption and desorption of a reactive azo dye by pumpkin husk, Environ. Sci. Pollut. Res. 21 (2014) 5086–5097.
[42] H. Chen, J. Zhao, J. Wu, G. Dai, Isotherm, thermodynamic, kinetics and adsorption mechanism studies of methyl orange by surfactant modified silkworm exuviae, J. Hazard. Mater. 192 (2011) 246–254.
[43] N.M. Mahmoodi, B. Hayati, M. Arami, C. Lan, Adsorption of textile dyes on Pine Cone from colored wastewater: Kinetic, equilibrium and thermodynamic studies, Desalination 268 (2011) 117–125.